DOI: 10.1111/ede.12270

RESEARCH

WILEY EVOLUTION & DEVELOPMENT

The evolution of selector gene function: Expression dynamics and regulatory interactions of *tiptop/teashirt* across Arthropoda

Logan E. March | **Rachel M. Smaby** | **Emily V. W. Setton** | **Prashant P. Sharma**

Department of Integrative Biology, University of Wisconsin-Madison, Madison, Wisconsin

Correspondence
Department of Integrative Biology, University of Wisconsin-Madison, 352 Birge Hall, 430 Lincoln Drive, Madison, WI 53706, USA.
Email: prashant.sharma@wisc.edu

Funding information
Division of Integrative Organismal Systems, Grant number: IOS-1552610

The transcription factors *spineless* (*ss*) and *tiptop/teashirt* (*tio/tsh*) have been shown to be selectors of distal appendage identity in an insect, but it is unknown how they regulate one another. Here, we examined the regulatory relationships between these two determinants in the milkweed bug *Oncopeltus faciatus*, using maternal RNA interference (RNAi). We show that *Ofas-ss* RNAi embryos bear distally transformed antennal buds with heterogeneous *Ofas-tio/tsh* expression domains comparable to wild type legs. In the reciprocal experiment, *Ofas-tio/tsh* RNAi embryos bear distally transformed walking limb buds with ectopic expression of *Ofas-ss* in the distal leg primordia. These data suggest that *Ofas-ss* is required for the maintenance of *Ofas-tio/tsh* expression in the distal antenna, whereas *Ofas-tio/tsh* represses *Ofas-ss* in the leg primordia. To assess whether expression boundaries of *tio/tsh* are associated with the trunk region more generally, we surveyed the expression of one myriapod and two chelicerate *tio/tsh* homologs. Our expression survey suggests that *tio/tsh* could play a role in specifying distal appendage identity across Arthropoda, but Hox regulation of *tio/tsh* homologs has been evolutionarily labile.

1 | INTRODUCTION

Arthropod appendages exhibit tremendous diversity, with structures that range from the powerful pincers of scorpions to the gracile pleopods of malacostracan crustaceans. Underpinning this considerable diversity is a conserved set of genes that pattern appendage identity during embryogenesis. The proximo-distal axis of panarthropod appendages in particular is patterned by a suite of transcription factors whose positional relationships are broadly conserved (Abu-Shaar & Mann, 1998; Cohen, Brönner, Küttner, Jürgens, & Jäckle, 1989; Dong, Chu, & Panganiban, 2001; Dong, Dicks, & Panganiban, 2002; Janssen, Eriksson, Budd, Akam, & Prpic, 2010; Mardon, Solomon, & Rubin, 1994; Panganiban et al., 1997; Panganiban, Nagy, & Carroll, 1994; Panganiban, Sebring, Nagy, & Carroll, 1995; Prpic, Janssen, Wigand, Klingler, & Damen, 2003; Schoppmeier & Damen, 2001; Sharma, Schwager, Extavour, & Giribet, 2012a). Similarly, the establishment of arthropod appendage types along the antero-posterior axis is achieved by the activity of trunk Hox genes throughout the phylum (Emerald & Cohen, 2004; Liubicich et al., 2009; Martin et al., 2016; Pavlopoulos et al., 2009; Pechmann, Schwager, Turetzek, & Prpic, 2015; Struhl, 1982a; Struhl & White, 1985) and by *homothorax* (Casares & Mann, 1998; Ronco et al., 2008; Sharma et al., 2015).

Exceptions to this general trend of evolutionary conservation abound, however. Among the most intriguing of these exceptions are those subsets of patterning genes whose expression and function have diverged across arthropods, in a manner reflecting phylogenetic relationships. For example, the flagellar territory of the antenna is associated with strong and early expression of the distal antennal determinant *spineless* (*ss*) across mandibulate arthropods, whereas chelicerates (arthro-pods lacking an antenna) lack a comparable *ss*

 © 2018 Wiley Periodicals, Inc.

expression domain in their corresponding head appendage (Duncan, Burgess, & Duncan, 1998; Setton et al., 2017; Struhl, 1982b).

One such case of functional divergence across arthropod species is the zinc finger transcription factor *teashirt* (*tsh*) and its paralog *tiptop* (*tio*). In the fruit fly *Drosophila melanogaster*, *tsh* is required for trunk identity; *tsh* loss-of-function mutants bear shorter larvae, disrupted denticle belts on trunk segments, and ectopic head-specific cuticle in the trunk region. These loss-of-function mutants also exhibit ectopic expression of the Hox gene *Sex combs reduced* (*Scr*) in the thorax (Fasano, Röder, Coré, Alexandre, & Vola, 1991; Röder, Vola, & Kerridge, 1992). Null mutants of various Hox genes that specify trunk identity also disrupt *tsh* expression, whereas ectopic misexpression of *tsh* in the anterior segments induces denticle belts (a trunk landmark) in the head. Taken together, these data have been interpreted to mean that *tsh* and Hox genes act in parallel to pattern trunk identity (Röder et al., 1992). The defects observed in *tsh* loss-of-function mutants are exacerbated when *tsh* and *tio* functions are abrogated simultaneously, and *tio* can nearly rescue *tsh* null mutants, suggesting a conserved function of the ancestral *tio/tsh* gene copy as a trunk selector (Denholm et al., 2013; Laugier, Yang, Fasano, Kerridge, & Vola, 2005; but see Shippy, Tomoyasu, Nie, Brown, & Denell, 2008). Additionally, *tsh* is required for the differentiation of stellate cells of the Malpighian tubules of *D. melanogaster* (Denholm et al., 2013).

In contrast to members of the genus *Drosophila*, a single homolog of the two genes ("*tio/tsh*", *sensu* Laugier et al., 2005) occurs in all other arthropods surveyed to date (Santos, Fonseca, Vieira, Vieira, & Casares, 2010; Shippy et al., 2008). Expression surveys have shown that the earliest domains of the ancestral insect *tio/tsh* homolog occur in the thoracic segments in embryonic stages immediately prior to, and during, the outgrowth of the limb buds (Herke, Serio, & Rogers, 2005; Peterson, Rogers, Popadic, & Kaufman, 1999; Shippy et al., 2008). Functional data for *tsh* homologs, however, are limited to two other insect species. In the flour beetle *Tribolium castaneum*, the *tio/tsh* homolog is required for proper growth and fusion of the labial limb buds, as well as the growth of the appendages, but this homolog does not exhibit any evidence of being a trunk selector (Shippy et al., 2008). It is also expressed in the primordia of the Malpighian tubules and later in stellate cells (Denholm et al., 2013; Shippy et al., 2008), but no renal phenotype is associated with *Tcas-tio/tsh* knockdown. In the milkweed bug *Oncopeltus fasciatus*, the single *tio/tsh* homolog has a separate peculiar phenotype, consisting of homeotic transformations of the distal legs to antennal identity (Herke et al., 2005); as with *T. castaneum*, no renal phenotype has been reported. Based on these data, the characterization of *tio/tsh* as a trunk selector across arthropods has been questioned and its function cannot be polarized on a phylogenetic tree (Shippy et al., 2008).

The distal leg selector function of *tio/tsh* in *O. fasciatus* is particularly intriguing because it has not been reported in any other arthropod. It was initially suggested that *Ofas-tio/tsh* and the Hox gene *Antennapedia* (*Antp*) may play different roles in specifying leg fate in comparison to *D. melanogaster*, as *Ofas-Antp* knockdown did not incur the classic homeotic leg-to-antenna transformations described in the fruit fly (Herke et al., 2005). However, Angelini et al. (2005) separately showed that *Ofas-Antp* does specify leg fate, albeit in small subset (<15%) of severe RNAi phenotypes. Nevertheless, the regulatory interactions between *Ofas-tio/tsh* and other appendage selector genes were not subsequently explored, and it is therefore unknown how this function of *Ofas-tio/tsh* has been integrated with more conserved elements of fate specification gene regulatory networks (GRNs).

Recently, we have shown that *Ofas-ss* knockdown results in distal antenna-to-leg transformation, implying evolutionary conservation of distal antennal selector function with respect to the fruit fly and flour beetle's *ss* homologs (Setton et al., 2017). Here, to examine the regulatory interaction between *tio/tsh* and *ss* in *O. fasciatus*, we performed knockdowns of each selector and assayed the expression of the other in RNAi embryos.

In our previous study, we had also surveyed the expression pattern of *ss* homologs in non-insect arthropods to demonstrate that the strong expression domain of insect *ss* in the distal antenna is found in all antennal types of mandibulates (arthropods with antennae), but not in chelicerates (which lack antennae). In the case of *tio/tsh*, it is not known how expression boundaries vary across arthropod bauplans beyond insects. The insect thorax corresponds to the anterior-most trunk segments across all Mandibulata (myriapods and pancrustaceans), but in Chelicerata, the sister group of Mandibulata, the walking legs occur more anteriorly than in mandibulates (Figure 1a). To facilitate direct comparisons of *ss* and *tio/tsh* evolutionary dynamics across the arthropod tree of life, we generated the first expression data for myriapod and chelicerate *tio/tsh* homologs.

2 | MATERIALS AND METHODS

2.1 | Animal husbandry

A colony of *Oncopeltus fasciatus* was maintained following the procedure described by Liu and Kaufman (2009a). Briefly, the insects were housed at 26°C with dry cotton substrate for egg laying, and provisioned with ground sunflower seeds and a water source. Embryo collection and fixation also followed the protocols of Liu and Kaufman (2009b).

A colony of the stone centipede *Lithobius atkinsoni* was maintained at 26°C. Husbandry and embryo collection

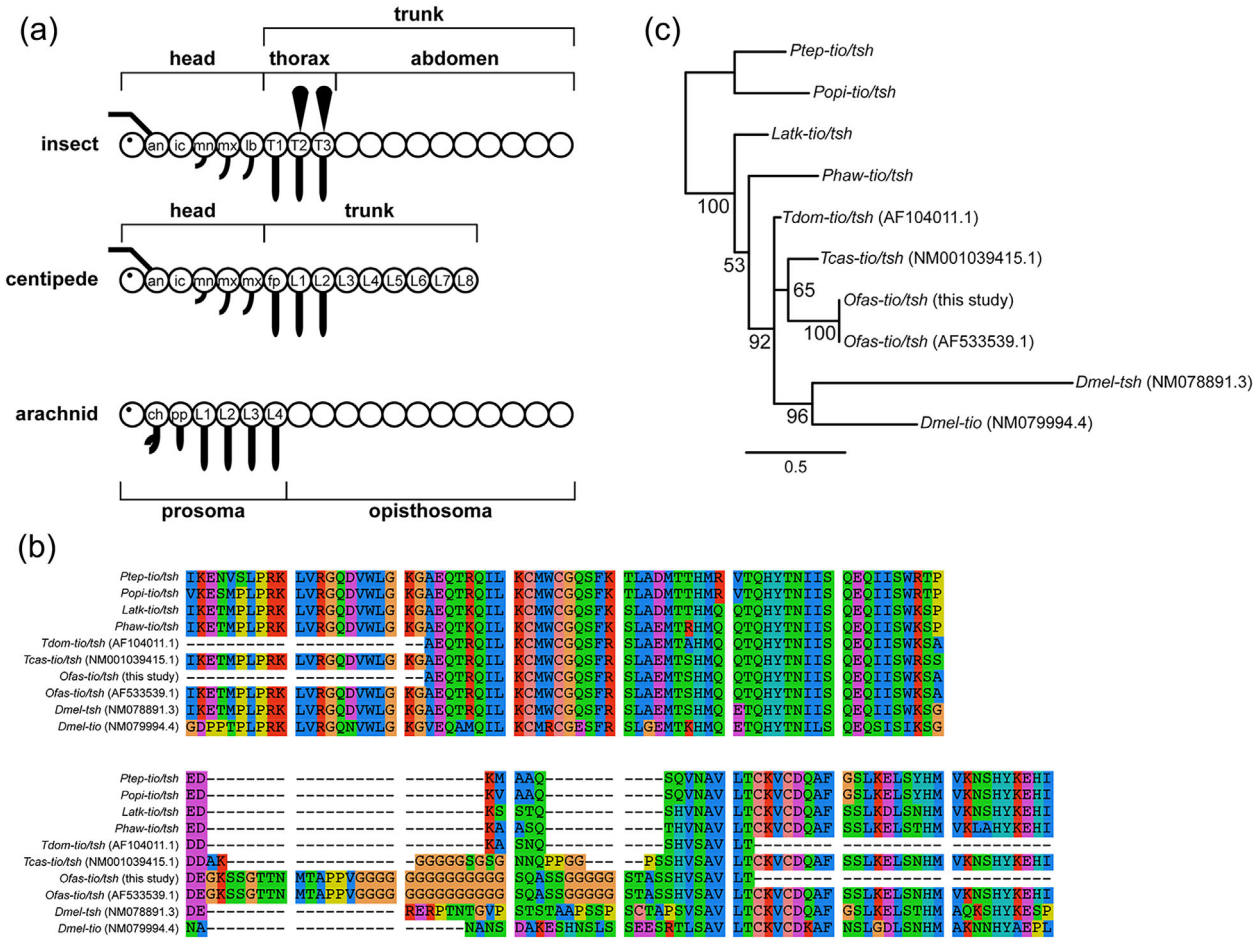

FIGURE 1 (a) Schematics of insect and arachnid bauplans, indicating tagmata, appendage types, and putative alignment of segments. Segmental abbreviations for insect and centipede: an: antennal; fp, forcipule; ic: intercalary; mn: mandibular; mx: maxillary; lb: labial; T1: first thoracic segment. Segmental abbreviations for arachnid: ch: cheliceral; pp: pedipalpal; L1: first walking leg; O1: first opisthosomal. (b) Portion of multiple sequence alignment of *tio/tsh* homologs, indicating conserved regions. (c) Maximum likelihood tree topology of *tio/tsh* homologs across Arthropoda ($\ln L = -3540.714$). Terminals include accession numbers for previously sequenced data. Numbers on nodes indicate bootstrap resampling frequencies. Taxonomic abbreviations: Dmel, *Drosophila melanogaster*; Tcas, *Tribolium castaneum*; Ofas, *Oncopeltus fasciatus*; Tdom, *Thermobia domestica*; Phaw, P*arhyale hawaiensis*; Latk, *Lithobius atkinsoni*; Ptep, *Parasteatoda tepidariorum*; Popi, *Phalangium opilio*

followed our previously published protocols (Setton et al., 2017; Setton & Sharma, 2018). Tissues were fixed in a 150 µl bubble of 4% PFA in 1× PBS, supplemented with heptane for 1 hr. Embryos were removed from the vitelline membrane and yolk prior to dehydration in methanol.

Colonies of the cobweb spider *Parasteatoda tepidariorum* and the harvestman *Phalangium opilio* were maintained at 26°C. Husbandry, embryo collection, and tissue fixation followed previously published protocols (Akiyama-Oda & Oda, 2003; Sharma, Schwager, Extavour, & Giribet, 2012b).

2.2 | Bioinformatics and probe synthesis

A fragment of the *O. fasciatus tio/tsh* ortholog was identified from the genome project of this species (Panfilio et al., 2017), using the 300-bp GenBank sequence of *Ofas-tio/tsh* identified by (Herke et al., 2005) as the query sequence. Gene specific primers were designed for a larger, 776-bp fragment of *Ofas-tio/tsh*, and PCR products were cloned using the TOPO® TA Cloning® Kit with One Shot® Top10 chemically competent *Escherichia coli* (Invitrogen, Carlsbad, CA) following the manufacturer's protocol. Sequence identities verified by Sanger sequencing with M13 universal primers.

A single 3708-bp fragment of the *L. atkinsoni tio/tsh* ortholog was identified from the developmental transcriptome of this species (Setton et al., 2017), using the *Drosophila melanogaster tio* and *tsh* sequences as queries. Gene specific primers were designed for a 991-bp fragment of *Latk-tio/tsh* with an added linker sequence (5′-ggccgcgg-3′ for the forward primer end and 5′-cccggggc-3′ for the reverse primer).

A single 1876-bp fragment of the *P. opilio tio/tsh* ortholog was identified from the developmental transcriptome of this species (Sharma, Kaluziak, et al., 2014a), using the *Drosophila melanogaster tio* and *tsh* sequences as queries. Gene specific primers were designed for a 777-bp fragment of this gene with an added linker sequence (5′-ggccgcgg-3′ for the forward primer end and 5′-cccggggc-3′ for the reverse primer).

A single 2906-bp fragment of *P. tepidariorum tio/tsh* ortholog was identified from the developmental transcriptome and genome of this species (Posnien et al., 2014; Schwager et al., 2017), using the *Drosophila melanogaster tio* and *tsh* sequences as queries. Gene specific primers were designed for a 794-bp fragment of *Ptep-tio/tsh*. Amplification and cloning followed the same procedures as for *O. fasciatus*.

Orthology was inferred using multiple sequence alignment of peptide sequences with MUSCLE v. 3.8.31 (Edgar, 2004). Additional sequence data included were selected to represent major lineages of Mandibulata, namely, from the amphipod crustacean *Parhyale hawaiensis* (Kao et al., 2016). Phylogenetic inference under maximum likelihood was conducted with RAxML v. 8.0 (Stamatakis, 2014) under an LG model (Le, Dang, & Gascuel, 2012) and correction for a discrete gamma distribution, with 500 independent starts and 500 bootstrap replicates (Stamatakis, Hoover, & Rougemont, 2008). The multiple sequence alignment and gene tree topology are provided as Supplementary Files S1 and S2, respectively.

Probe synthesis was conducted using components of the MEGAscript® T7 kit (Ambion/Life Technologies, Grand Island, NY). Sense and anti-sense probes were synthesized using T7 and T3 RNA polymerases (Life Technologies) and precipitated with ammonium acetate, following the manufacturer's protocol.

All primer sequences and amplicon lengths are provided in Supplementary File S3.

2.3 | Whole mount in situ hybridization

For *Ofas-ss* experiments, we used the longer gene fragment that we previously isolated and cloned into plasmid for parental RNAi (Setton et al., 2017).

Whole mount in situ hybridization for *O. fasciatus* was performed as described previously (Liu and Kaufman, 2009c). Hybridization was performed at 55°C with probe stock concentrations of 30 ng/μl (*Ofas-ss*) or 50 ng/μl (*Ofas-tio*), prior to 1:10 dilution in hybridization solution. Staining reactions for detection of transcripts in NBT/BCIP lasted between 0.5 (*Ofas*-ss) and 12 hr (*Ofas-tio*) at room temperature. Embryos were subsequently rinsed with 1× PBS + 0.1% Tween-20 to stop the reaction, counterstained with 10 μg/ml Hoechst 33342 (Sigma–Aldrich, St. Louis, MO) to label nuclei, post-fixed in 4% formaldehyde in 1× PBS + 0.1% Tween-20, and stored at 4°C in glycerol.

In situ hybridization for *L. atkinsoni* followed modified protocols (Setton & Sharma 2018; Setton et al., 2017). In addition to performing in situs on whole embryos, the germbands of some living embryos were dissected from the yolk in PBST at a range of limb bud bearing stages (3 to 8, *sensu* Kadner & Stollewerk, 2004) prior to dehydration in methanol. Hybridization was performed at 65°C with probe stock concentrations of 425 ng/μl, prior to 1:10 dilution in pH 7.0 hybridization solution.

Whole mount in situ hybridization for *P. tepidariorum* and *P. opilio* followed previously published protocols (Akiyama-Oda & Oda, 2003; Sharma et al., 2012b). Hybridization was performed at 65°C with probe stock concentrations of 500 ng/μl, prior to 1:10 dilution in hybridization solution. Subsequent operations were identical to those described for *O. fasciatus*.

2.4 | Double-stranded RNA synthesis and parental RNA interference

Double-stranded RNA (dsRNA) was synthesized from PCR products derived from plasmid DNAs for *Ofas-ss* and *Ofas-tio*, using the MEGAscript® T7 kit (Ambion/Life Technologies) according to the manufacturer's protocol. The concentration of the resulting dsRNA product was measured using a Nanodrop One spectrophotometer and diluted to a working concentration of 2 μg/μl dsRNA in 1× *Tribolium* injection buffer.

Between 2 and 5 days after their final molt, virgin adult female *O. fasciatus* were injected with 5 μg dsRNA of either Ofas-ss ($N = 12$ females) or *Ofas-tio/tsh* ($N = 12$ females). An equal volume of 1× *Tribolium* injection buffer was used as the negative control ($N = 8$ females). Injected females were stored in individual petri dishes and given water, cotton substrate for egg laying, crushed sunflower seeds for food, and a soaked cotton plug with deionized water. Two days after injection, females were mated by the addition of one male to each dish. The first eight clutches from each female were collected and placed in an incubator at 26°C for 72–78 hr after egg laying (hAEL).

A subset of embryos was harvested and fixed 72 hr after egg-laying (AEL), as previously described (Liu & Kaufman, 2009b). Briefly, embryos were boiled for 1 min in 300 μl of deionized water, snap cooled on ice, and rapidly washed with methanol to facilitate removal of chorions. Thereafter, the embryos were agitated in heptane supplemented with 4% formaldehyde in PBS for 45 min, and dehydrated into methanol for storage at −20°C. For each clutch, approximately half of the eggs were not fixed, and instead left in the incubator until hatching to assess knockdown penetrance.

Hatchlings were preserved in 70% ethanol and stored at −20°C.

2.5 | Imaging

Stained embryos were mounted in glycerol and photographed using a Nikon SMZ25 fluorescence stereomicroscope mounted with either a DS-Fi2 digital color camera or a Q-Imaging digital monochrome camera, driven by Nikon Elements software. Leg mounts prepared in glycerol, as well as flat mounts of whole embryos, were imaged using an Olympus DP70 color camera mounted on an Olympus BX60 epifluorescence compound microscope. For flat mounts, a series of images (3–5) was taken at regular intervals and the source images were focus-stacked using the software Helicon Focus v. 6.7.1. under the depth map algorithm.

Scanning electron microscopy (SEM) was conducted using a FEI Quanta 200. Selected hatchlings of *O. fasciatus* were gradually dehydrated into ethanol. Appendages (legs and antennae) were removed at the body wall and affixed to adhesive carbon tabs mounted on SEM stubs and sputter coated for 90 s using a platinum-palladium target. Images were captured using a voltage of 15 kV and a spot size of 3.0.

3 | RESULTS

3.1 | Identification of *tio/tsh* orthologs

After culling 5′ and 3′ hanging ends, the multiple sequence alignment of *tio/tsh* homologs retrieved from transcriptomic and genomic databases consisted of 367 amino acid sites (fragment shown in Figure 1b). The maximum likelihood tree recovered the expected tree topology of *tio/tsh* orthologs *sensu* Santos et al. (2010), with a grouping of the *tio* and *tsh* paralogs of *D. melanogaster*; the rest of the gene tree reflected the basal phylogeny of arthropods (monophyly of the nodes Mandibulata, Pancrustacea, and Hexapoda; Figure 1c). The placement of the firebrat homolog (*Tdom-tio/tsh*) was uncertain, due to the incompleteness of the available sequence.

3.2 | Parental RNA interference in *O. fasciatus*

Eleven of the 12 *O. fasciatus* females injected with *Ofas-tio*-dsRNA survived to produce clutches. Of these, six consistently produced eggs that displayed distal leg defects, consisting of loss of segments at the distal termini and the appearance of setae characteristic of wild type antennae (sensory pegs; Figure 2). These six females produced 125 eggs that hatched successfully, and of these, 99.2% ($N = 124/125$) expressed the distal leg defects described by Herke et al. (2005). All head appendages were of wild-type morphology, and no homeosis pertaining to the trunk (body) segments was observed. We interpret the range of this phenotypic spectrum to be the same as that generated previously by Herke et al. (2005) using an embryonic RNAi approach, but with a higher proportion of specific defects in surviving hatchlings.

Penetrance of *Ofas-ss* dsRNA has been described by us in detail recently (Setton et al., 2017), and was improved in the present study, with 100% of embryos of females injected with a 798-bp fragment of *Ofas-ss* displaying distal antenna-to-leg transformations ($N > 250$; Figures 2 and 3g–i).

3.3 | Inference of *Ofas-tio/tsh* regulation

To infer how *Ofas-tio/tsh* is regulated by *Ofas-ss*, we assayed expression of *Ofas-tio/tsh* in a sample of embryos exhibiting reduction of *Ofas-ss* expression at 72–78 hAEL (as inferred from the phenotypes of the rest of the clutch upon hatching).

In embryos of buffer-injected (negative control) females, *Ofas-tio/tsh* was strongly expressed in the presumptive distal flagellum of the antenna, and weakly in the proximal and medial antennal regions (Figure 3c), whereas in the walking leg, *Ofas-tio/tsh* was heterogeneously expressed as rings, with notable absence of *Ofas-tio/tsh* in the distal tip of the leg ($N = 13/13$) (Figure 3f); these patterns are consistent with wild type expression (Supplementary Figure S1; Herke et al., 2005).

By contrast, in embryos exhibiting *Ofas-ss* RNAi phenotypes, expression of *Ofas-tio/tsh* is lost in the distal-most territory of the antenna, with only weak expression of *Ofas-tio/tsh* retained proximally ($N = 14/17$) (Figures 3h and 3i). Morphologically, the inflected distal bulb of the homeotically transformed distal antenna corresponds to the second tarsomere identity. The remainders of the clutches surveyed for *Ofas-tio/tsh* expression were permitted to hatch, and 100% of hatchlings from these subsets yielded severe *Ofas-ss* RNAi phenotypes *sensu* Setton et al. (2017), as shown in Figure 3g.

In 100% of *Ofas-ss* RNAi embryos surveyed ($N = 17$), wild type expression of *Ofas-tio/tsh* was observed in the walking legs and the rest of the body (not shown; Figure S1).

3.4 | Inference of *Ofas-ss* regulation

To infer how *Ofas-ss* is regulated by *Ofas-tio*, we assayed expression of *Ofas-ss* in embryos exhibiting reduction of *Ofas-tio/tsh* expression at 72–78 hAEL. In embryos of buffer-injected females, *Ofas-ss* was expressed only in the distal antennal buds ($N = 22/22$; Figure 4a), reflecting the wild-type condition described previously (Setton et al., 2017).

In 100% of *Ofas-tio/tsh* RNAi embryos ($N = 28/28$), expression of *Ofas-ss* comprised the distal antennal buds as well as the distal tips of all six walking legs (Figure 4d–f). Consistent with the segmentation phenotype previously described from hatchlings (Figures 4b and 4c; Herke et al.,

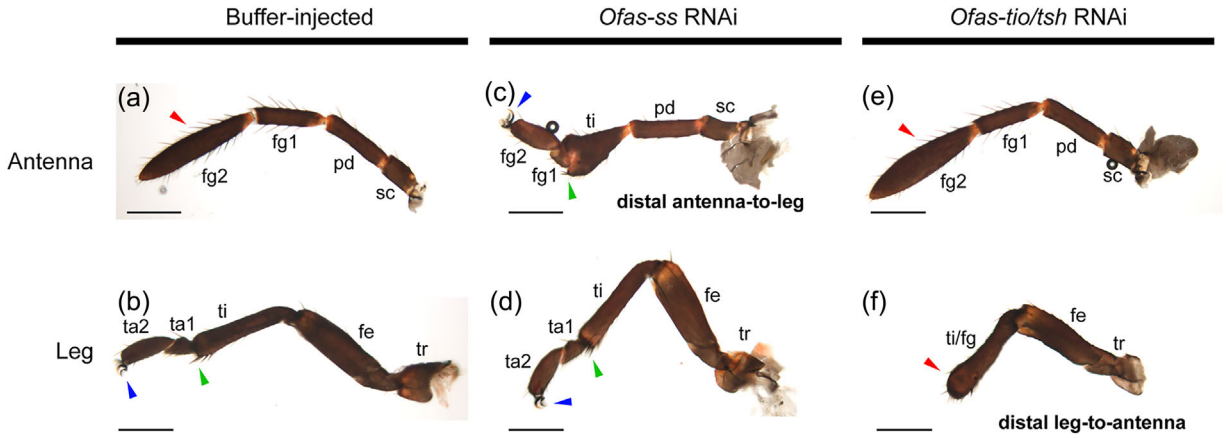

FIGURE 2 Appendage mounts of first instar *O. fasciatus* control (a and b), *Ofas-ss*-dsRNA (c and d), and *Ofas-tio*-dsRNA (e and f) injected embryos. Bristle pattterns of the antenna are indicated by red arrowheads. Tarsal claws and tibial setae are indicated by blue and green arrowheads, respectively. Strong *Ofas-ss* RNAi phenocopies bear wild type legs (d) but distal antennae are transformed into leg structures (c). Inversely, strong *Ofas-tio/tsh* RNAi phenocopies bear wild-type antennae (e), but bear distal segmentation defects and are distally transformed into antennal identity. fe, femur; fg1: first flagellomere; fg2: second flagellomere; pd: pedicel; sc: scape; ta1: first tarsomere; ta2: second tarsomere; ti: tibia; tr: trochanter. Scale bar: 500 μm

2005), *Ofas-tio/tsh* RNAi embryos also exhibited shorter T1-T3 appendages, relative to negative control embryos of equivalent age (Figure 4f). No other appendages were discernibly affected by the knockdown with respect to either morphology or ectopic *Ofas-ss* expression.

3.5 | Expression of myriapod *tio/tsh*

Embryos of the centipede *L. atkinsoni* expressed *Latk-tio/tsh* comparably to insect counterparts at corresponding stages (Figure 5). The strongest expression in limb bud stage embryos was observed in the walking legs, the maxillae, the labrum, and the distal antenna, but not the mandible (stage 4). In addition, expression is also detected in the posterior terminus immediately anterior to the proctodeum (Figure 5a). During blastokinesis (stage 6), expression is intensified in the posterior terminus as well as the outgrowing limb buds. Expression in the mandible is still diminished compared to the other limb buds (Figure 5b). In the last stages where we could perform in situ hybridization (stage 7, just prior to onset of cuticle formation), these expression domains were retained, but we did not observe heterogeneous expression domains along the PD axis of the leg, as in insects (Figure 5c; compare to Figure 3f, S1).

3.6 | Expression of arachnid *tio/tsh* homologs

During embryogenesis of the harvestman *P. opilio*, the earliest expression of *Popi-tio/tsh* is observed in stages corresponding to the segmentation of the prosoma (stage 8; Figures 6a and 6b). At this stage, expression of *Popi-tio/tsh* occurs in the limb bud primordia of the pedipalps and four pairs of walking legs, as well as in the first opisthosomal segment (O1). The expression is significantly weaker in the opisthosomal segment than in the pedipalpal and walking leg primordia. In later stages (stage 10), the expression domain of *Popi-tio/tsh* expands to include most of the germband, including the ventral ectoderm, the eye field primordia, and the entire opisthosoma (Figure 6c–e). In this stage, the strongest expression continues to be observed in the pedipalps and walking legs, and elongation of limb bubs is associated with a complex, heterogeneous expression pattern, consisting of a ring at the base of the limb bud (Figure 6d), as well as concentration of *Popi-tio/tsh* transcripts in the distal terminus of these five appendage pairs (Figure 6e). Notably, expression in the cheliceral limb bud consists only of weak expression in the distal tip of the PD axis; no rings of expression are observed at the intersection of the appendage and the body wall during embryogenesis, and cheliceral expression of *Popi-tio/tsh* is consistently weaker than in other appendages (Figure 6e).

Expression patterns of the *tio/tsh* homolog in the spider *P. tepidariorium* are broadly conserved with respect to the harvestman (Figure 6f–i). By stage 9.1, expression of *Ptep-tio/tsh* is most concentrated in the pedipalpal and walking leg limb buds (Figures 6f and 6h), with weaker expression throughout the opisthosoma (Figure 6f); no expression is observed in the cheliceral limb buds in this stage (Figures 6f and 6g). In later stages (stage 10.2), *Ptep-tio/tsh* expression is additionally strongly expressed in the limb-like primordia of the book lungs and both pairs of spinnerets, with additional expression domains in the ventral ectoderm (Figure 6i).

As negative controls, we tested for expression of sense probes in embryos of both arachnid species and the centipede. In all cases, only observed background staining (data

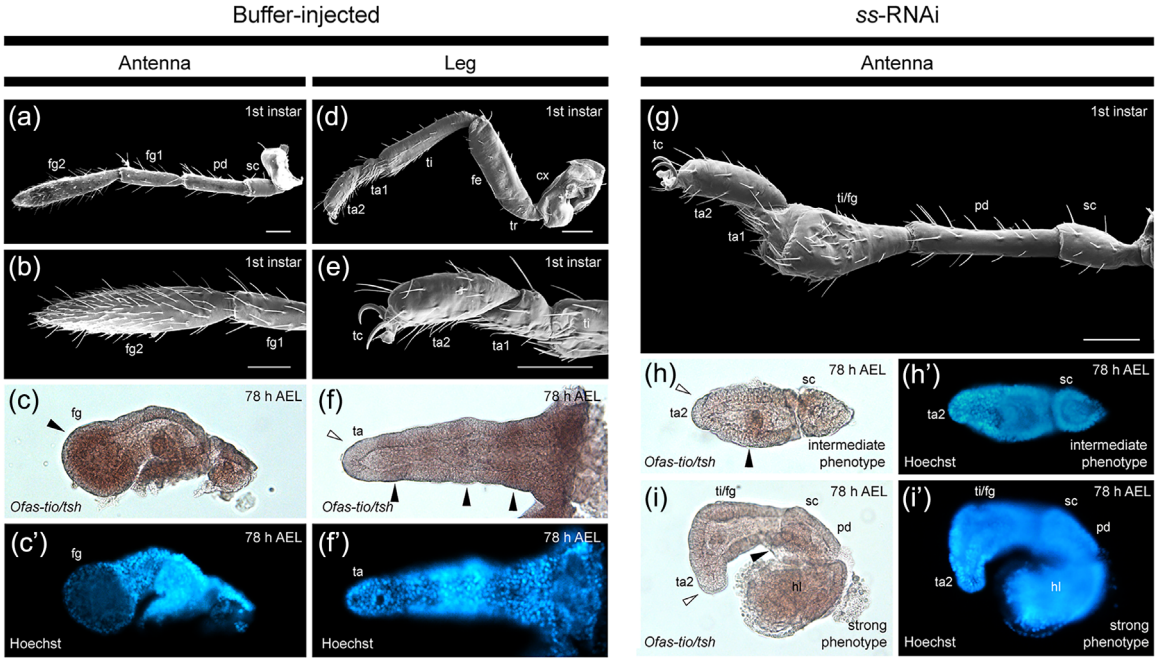

FIGURE 3 *Ofas-ss* is required for distal expression of *Ofas-tio/tsh* in the antenna. (a) SEM micrograph of the antenna of a wild-type first instar (hatchling). (b) Detail of distal antenna of a wild-type first instar. (c) In buffer-injected embryos at 78 hAEL, *Ofas-tio/tsh* is strongly expressed in the distal embryonic antenna (black arrowhead), and weakly in the proximal territories corresponding to the presumptive scape and pedicel. (d) SEM image showing the leg of a wild-type first instar (hatchling). (e) Detail of the distal end wild-type leg from a first instar hatchling. (f) At 78 hAEL, *Ofas-tio/tsh* is expressed heterogeneously along the proximo-distal axis of the walking leg. Weak expression indistinguishable from background occurs in the distal terminus (white arrowhead), alternating with bands of strong expression (black arrowheads). (g–i) *Ofas-ss*-RNAi embryos undergo homeotic distal antenna-to-leg transformations. (g) SEM micrograph of an antenna from an *ss*-hatchling, showing the distal antennae-to-leg transformation. (h) In embryos displaying intermediate phenocopies of *Ofas-ss*-RNAi at 78 hAEL, expression of *Ofas-tio/tsh* is greatly reduced at the distal terminus (white arrowhead), though some expression is still observed medially (black arrowhead). (i) In strong phenocopies of *Ofas-ss*-RNAi, embryos at 78 hAEL show no expression of *Ofas-tio/tsh* in the distal tip (white arrowhead), and weak expression more proximally (black arrowhead). The distally transformed region bears a small bulb that corresponds to the presumptive second tarsomere identity in this transformed region. Here, part of the embryonic head has been retained to show true expression signal in the head lobe for comparison. (c', f', h', i') Counterstaining of (c, f, h, i) with Hoechst 33342. hl, head lobe; ta: tarsus; other abbreviations as in Figure 2. Scale bars: 100 μm

available upon request). These results suggest specific binding by the antisense riboprobe.

4 | DISCUSSION

The fate specification mechanism of the insect distal antenna has been shown to be conserved with respect to the involvement of the distal antennal selector gene *spineless* (*ss*) and its interactions with the proximo-distal axis patterning genes *homothorax* (*hth*) and *Distal-less* (*Dll*), as inferred from available data from three insect species (Duncan et al., 1998; Emmons, Duncan, & Duncan, 2007; Kuzin, Doszhanov, & Mazo, 1997; Setton et al., 2017; Shippy, Yeager, & Denell, 2008; Struhl, 1982b; Toegel, Wimmer, & Prpic, 2009). The hemimetabolous insect *O. fasciatus* is nevertheless unusual in two respects. First, in contrast to *D. melanogaster* and *T. castaneum*, the tarsal field of the *O. fasciatus* walking leg does not express *ss* in wild-type embryos, and knockdown of *ss* has no effect on this region of the walking leg (Setton et al., 2017). Second, only in *O. fasciatus* does the *tio/tsh* homolog play a role as a distal leg selector (Herke et al., 2005); in *D. melanogaster* and *T. castaneum*, *tio/tsh* paralogs have other functions that pertain to patterning trunk identity, the Malpighian tubules, and/or leg and body wall growth, but these paralogs are not involved in distal leg fate specification (Denholm et al., 2013; Laugier et al., 2005; Shippy et al., 2008; Tomoyasu, Arakane, Kramer, & Denell, 2009; Wang, Tindell, Yan, & Yoder, 2013).

Toward understanding the relationship between *tio/tsh* and *ss* in *O. fasciatus*, we performed reciprocal knockdown experiments of each gene and assayed the resulting expression of the other.

4.1 | *ss* is required for maintenance of *tio/tsh* expression in the distal antenna of *O. fasciatus*

Our previous work has shown that the effect of *ss* loss of function is restricted to the developing antenna in *O. fasciatus*

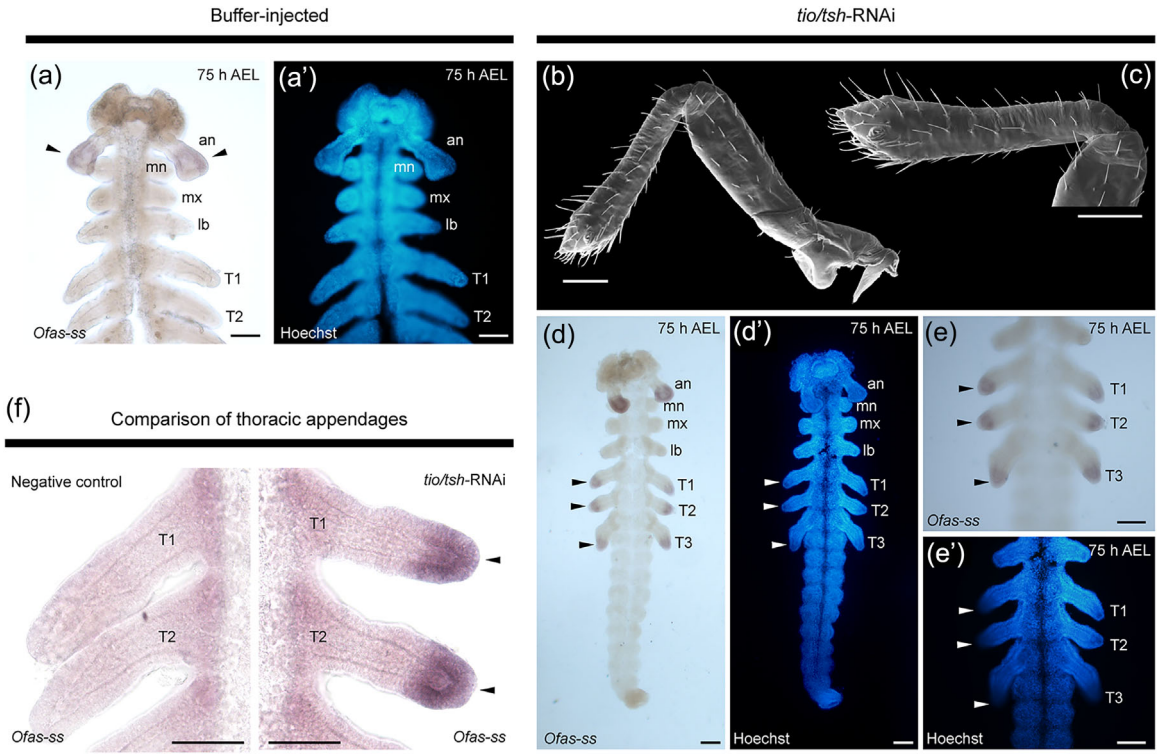

FIGURE 4 *Ofas-tio/tsh* suppresses distal expression of *Ofas-ss* in the legs. (a) Wild-type expression of *Ofas-ss* is restricted to the antennal limb buds. Note lack of expression in walking leg termini. (b–d) *Ofas-tio/tsh*-RNAi embryos undergo homeotic distal leg-to-antenna transformations (b) SEM micrograph of the leg of a strong *Ofas-tio/tsh*-RNAi phenotype at first instar. (c) Detail of distal terminus of the transformed appendage shown in (b). (d) Embryo of a strong *Ofas-tio/tsh*-RNAi phenotype at 75 hAEL, showing ectopic expression of *Ofas-ss* in the distal termini of T1-T3 (arrowheads). (e) Detail of thorax of embryo shown in (d). (f) Comparison of T1 and T2 legs of wild-type and strong *Ofas-tio/tsh*-RNAi phenotype at 75 hAEL, showing ectopic *Ofas-ss* expression in distal termini (arrowheads) as well as shorter appendages upon RNAi. (a', d', e') Counterstaining of (a, d, e) with Hoechst 33342. Abbreviations as in Figure 2. Scale bars: 100 μm

(Setton et al., 2017). Our results herein revealed that the homeotic transformation of distal antennal identity associated with RNAi against *Ofas-ss* results in the diminution of *Ofas-tio/tsh* expression in the antennal limb buds. Expression of *Ofas-tio/tsh* elsewhere in the germband was not discernibly affected.

The altered expression pattern of *Ofas-tio/tsh* in the antennae of *Ofas-ss*-RNAi phenocopies is consistent with *Ofas-tio/tsh* expression in wild-type legs. In early stages of leg development, *Ofas-tio/tsh* is strongly expressed throughout the T1-T3, the maxillary, and the labial limb buds, but less strongly in the antennae and posterior terminus of the germband (Herke et al., 2005); Figure S1a). In later development, expression of *Ofas-tio/tsh* in the T1-T3 legs becomes heterogeneous, with an increase in the number of rings of expression through development along the leg's proximo-distal axis (Herke et al., 2005; Figure S1b and c). *Ofas-tio/tsh* is conspicuously absent from the distal terminus (the presumptive tarsal primordium) by 75 hAEL (Figure S1c). Apropos, the homeotic distal antenna-to-leg transformation induced by *Ofas-ss*-RNAi is associated with loss of expression from the distal terminus of the transformed antenna in both intermediate and strong phenocopies.

The positive regulatory interaction between *Ofas-ss* and *Ofas-tio/tsh* is unexpected, because loss-of-function experiments with *tio* and *tsh* orthologs have never revealed an antennal phenotype. It is therefore unclear what function, if any, *Ofas-tio/tsh* fulfills in the developing antennae. Within arthropods, recent work has revealed a role for *tio/tsh* orthologs in promoting cell proliferation in the anterior eye fields of *D. melanogaster* during postembryonic development (Datta, Weasner, & Kumar, 2011), but no selector function of *tio/tsh* in the antennal segment is known.

4.2 | *Tio/tsh* represses ss expression in distal leg of *O. fasciatus*

The *Ofas-tio/tsh* loss of function phenotype reported by Herke et al. (2005) comprised a homeotic distal leg-to-antenna phenotype. Drawing upon this datum, we tested the effect of *Ofas-tio*-RNAi on *Ofas-ss* expression, and showed herein that knockdown of *Ofas-tio/tsh* results in ectopic expression of *Ofas-ss* in the distal terminus of the T1-T3 appendages. No other appendages were observed to be affected, either through morphological examination (i.e., SEM imaging of hatchlings)

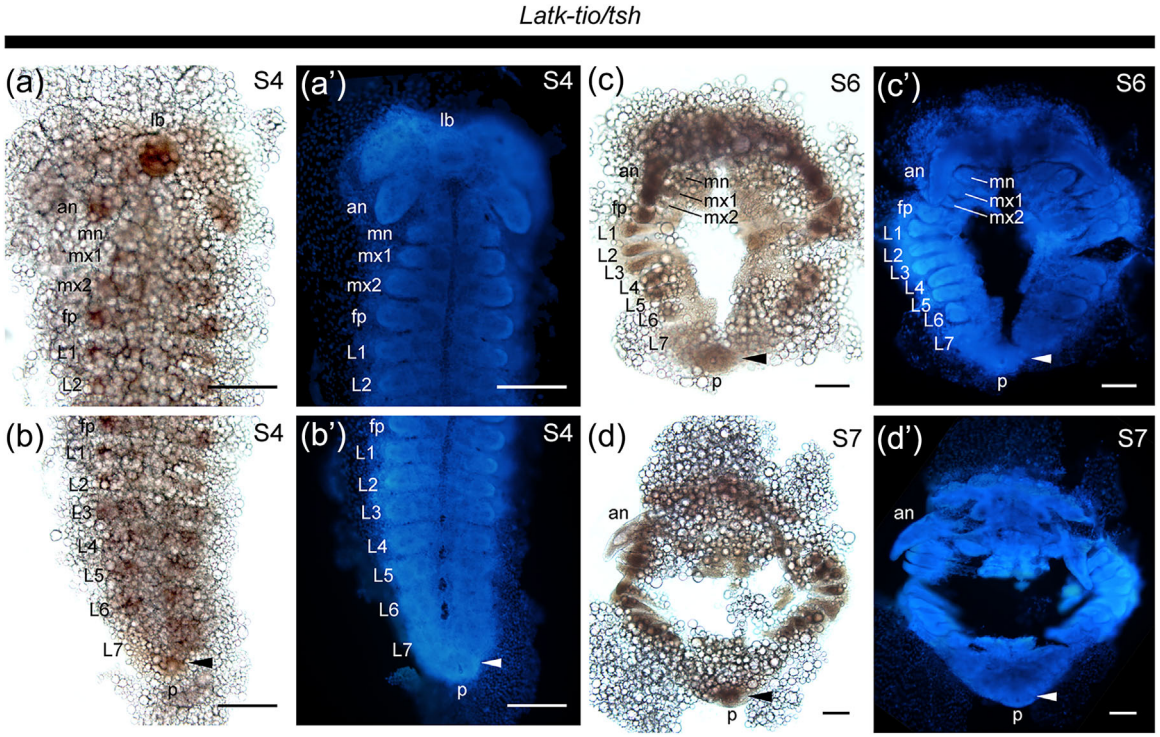

FIGURE 5 Expression of *tio/tsh* in the centipede. (a) Head and anterior trunk of a flat mounted embryo of *L. atkinsoni* at stage 4, showing expression of *Latk-tio/tsh* in the labrum and distal territories of all limb buds except the mandible. (b) Posterior trunk of same embryo shown in (a), showing expression of *Latk-tio/tsh* in the posterior terminus. (c) At stage 6 (blastokinesis), expression in the posterior terminus is more pronounced. (d) Expression in developing appendages and posterior terminus continues through stage 7, but heterogeneous expression of *Latk-tio/tsh* is not observed in the PD axis of the legs. (a'–d') Counterstaining of (a–d) with Hoechst 33342. lb, labrum. All other abbreviations as in Figure 1. All scale bars: 100 μm

or surveying embryonic gene expression. These results are consistent with the interpretation that *Ofas-tio/tsh* is a repressor of *Ofas-ss* in the developing T1-T3 appendages.

Interestingly, Herke et al. (2005) interpreted the function of *Ofas-tio/tsh* to mean a lineage-specific substitution of canonical Hox function, as their study also assessed the effect of *Ofas-Antp* knockdown via RNAi but did not obtain the characteristic leg-to-antenna transformation first observed in *D. melanogaster*. However, it was subsequently shown that *Ofas-Antp*-RNAi does incur homeotic leg-to-antenna transformation with low phenotypic penetrance (<15% of injected embryos) in this species (Angelini, Liu, Hughes, & Kaufman, 2005), but even in the strongest phenotypes, the tarsal claws were retained on the T1-T3 appendages (Figure 2i of Angelini et al., 2005). Our data are consistent with the interpretation that *Ofas-tio/tsh* may be part of the complex of genes that regulates pretarsal development in *O. fasciatus*, as hypothesized by Angelini et al. (2005).

The functional interactions presented herein are presently known only to apply to *O. fasciatus*, as *tio/tsh* loss-of-function phenotypes are not associated with distal leg selector function in any other insects. Beyond the three insects for which functional data are available, expression of *tio/tsh* had only been explored in an ametabolous insect, the firebrat *Thermobia domestica* (Peterson et al., 1999), and in the Malpighian tubules of the cricket *Gryllus bimaculatus* (Denholm et al., 2013). We therefore surveyed expression of *tio/tsh* homologs for the first time in exemplars of Chelicerata and Myriapoda.

4.3 | Evolution dynamics of *tio/tsh* and Hox expression domains in arthropods

The insect thorax corresponds to the anterior-most trunk segments across all Mandibulata (myriapods and pancrustaceans), but in Chelicerata, the sister group of Mandibulata, the walking legs occur more anteriorly than in mandibulates (Figure 1a). Walking legs are located on the fourth through the seventh body segments in Arachnida, and on the third through the seventh body segment in Xiphosura (horseshoe crabs), and on the fifth to the last segment in Pycnogonida (sea spiders). Myriapoda and Chelicerata thus have markedly different bauplans, to the point where defining the "trunk" of a chelicerate (much less homologizing this region to the mandibulate trunk) is nontrivial. The bauplans of these groups nevertheless lend themselves to a natural experiment to test the hypothesis that *tio/tsh* expression is associated with the corresponding leg-bearing territory of both groups.

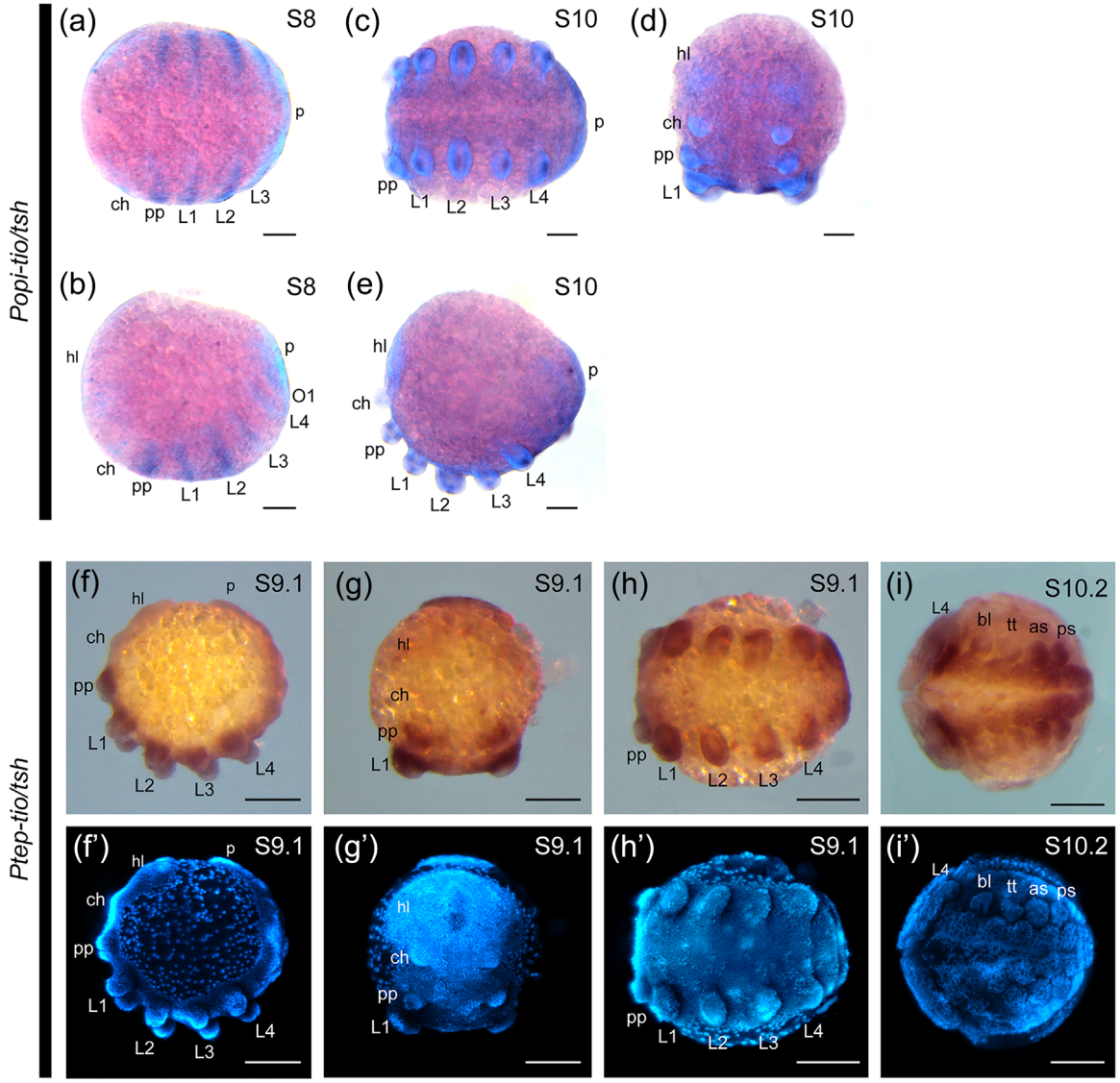

FIGURE 6 Expression of *tio/tsh* homologs in arachnids. (a–e) Whole mount in situ hybridization for *Popi-tio/tsh*. (f–i) Whole mount in situ hybridization for *Ptep-tio/tsh*. (a) Embryo of *P. opilio* at stage 8 in ventral view showing expression in the pedipalpal and walking leg segments. (b) Same embryo as in (a), in lateral view, additionally showing expression in the opisthosoma. (c) Stage 10 embryo in ventral view, showing concentration of *Popi-tio/tsh* transcripts in the pedipalps and walking legs, as well as the ventral ectoderm. (d) Same embryo as in (c), in frontal view, showing weak expression in the chelicerae. (e) Same embryo as in (c), in lateral view, showing complex expression pattern in the pedipalpal and walking leg buds; note limited expression in distal tip of chelicerae. (f) Embryo of *P. tepidariorum* at stage 9.1 in lateral view, showing strong expression of *Ptep-tio/tsh* in the pedipalpal and walking leg buds, as well as the opisthosoma. (g) Same embryo as in (f), in frontal view, showing lack of cheliceral and head lobe expression. (h) Same embryo as in (f), in ventral view, showing distinct expression in pedipalpal and walking leg buds. (i) Opisthosoma of *P. tepidariorum* at stage 10.2, showing concentration of *Ptep-tio/tsh* expression in the book lung and spinneret primordia. (f'–i') Counterstaining of (f–i) with Hoechst 33342. bl, book lung; tt, tubular tracheae; as, anterior spinneret; ps, posterior spinneret; p, posterior terminus. All other abbreviations as in Figure 1. Scale bars: 100 μm

Consistent with this prediction, we found that expression of *tio/tsh* homologs was uniformly associated with walking leg limb buds in all three non-insect species that we surveyed (Figures 5 and 6). In the centipede, expression of *tio/tsh* in limb bud stages was very similar to insect counterparts, with respect to the absence of expression in the mandible, clear expression in all remaining limb buds, and an expression domain in the posterior terminus. The last of these is worthy of further study; it may suggest comparable patterning of the Malpighian tubules in insects and myriapods (Shippy et al., 2008; Denholm et al., 2013), even though Malpighian tubules are clearly not homologous across the terrestrial arthropods and likely reflect convergent adaptation to life on land (like the tubular tracheae of insects, myriapods, and arachnids; Sharma, 2017). In chelicerates, strong expression of *tio/tsh* in the pedipalps and walking legs (in tandem with absence of

detectable expression in the anterior head and opisthosoma) suggest that *tio/tsh* expression boundaries are more closely associated with the location of appendages along the AP axis, rather than with other positional markers (e.g., the anterior expression domains of the Hox genes; Figure 7). The expression of *tio/tsh* in some opisthosomal organs (book lungs and both pairs of spinnerets) is a curious feature of later stages of spider embryogenesis (Figure 6i), but this may reflect their postulated serial homology to walking legs (Sharma, 2017).

Moreover, comparison of insect and arachnid expression domains is consistent with the interpretation that regulatory interactions between *tio/tsh* and the Hox genes have changed markedly during the evolution of insects and arachnids. Whereas *tsh* represses expression of the gnathal Hox genes *labial* (*lab*) and *Sex combs reduced* (*Scr*) in the trunk *D. melanogaster*, *tio/tsh* expression of both arachnids encompasses the expression domains of their *lab*, *Deformed* (*Dfd*), and *Scr* orthologs (Röder et al., 1992; Khadjeh et al., 2012; Sharma et al., 2012b). In addition, whereas trunk Hox genes like *Antp* and *Ubx* maintain *tsh* expression in the posterior compartment of specific *D. melanogaster* trunk segments, homologs of neither of these genes are expressed in the prosoma of arachnids during stages corresponding to leg fate specification (Khadjeh et al., 2012; Schwager et al., 2017; Sharma et al., 2012b; Sharma, Schwager, Extavour, & Wheeler, 2014b). Furthermore, the limited data available on Hox gene function in arachnids (e.g., *lab*-1, *Dfd-1*, *Antp-1*), in addition to expression patterns of centipede posterior Hox genes in the posterior trunk (the region correspond to the appendage-free insect abdomen), have shown that orthology of Hox genes does not correspond to homology of function between insects, centipedes, and arachnids (Hughes & Kaufman, 2002; Khadjeh et al., 2012; Pechmann et al., 2015). The evolution of *tio/tsh* and Hox expression domains thus appears to be decoupled.

The weak expression of *tio/tsh* in the chelicerae of arachnids, in contrast to the strong and heterogeneous expression patterns observed in the other appendages, are strongly reminiscent of the expression dynamics of *Ofas-tio/tsh*, which is similarly weakly expressed in the gnathos and forms rings of expression in the walking legs of both lineages (Figure 3f; S1). These patterns may be suggestive of conserved functions in appendage and/or body wall patterning between insects and arachnids, but this hypothesis awaits functional data in arachnid model systems for validation.

4.4 | Evolution of selector function in the *tio/tsh* gene family

One of the outstanding questions for arthropod evolution is whether *tio/tsh* is in fact a true trunk selector gene, as shown in *D. melanogaster* (Fasano et al., 1991; Röder et al., 1992).

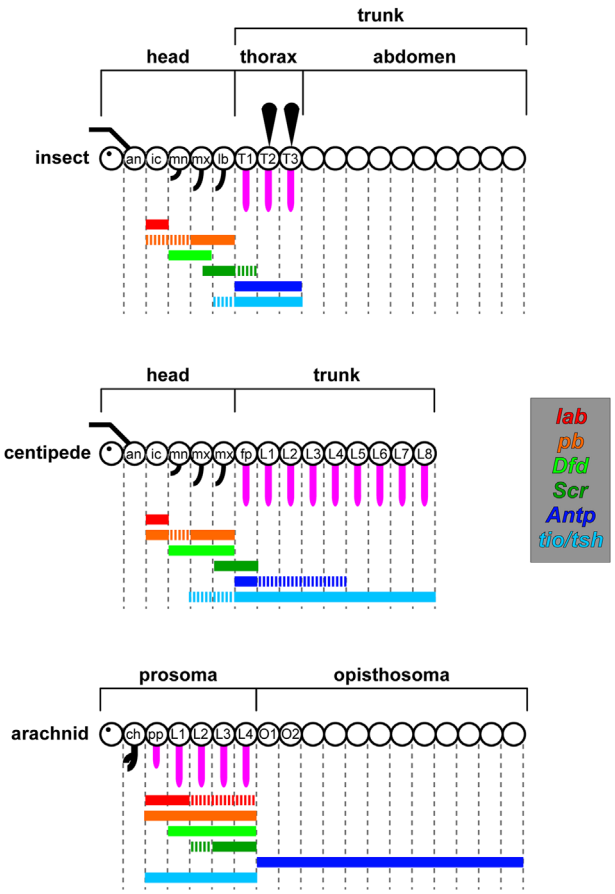

FIGURE 7 Schematic of insect, centipede, and arachnid bauplans, showing relative positions of *tio/tsh* and Hox gene expression boundaries. Abbreviations as in Figure 1

Beyond arthropods, *tio/tsh* homologs have been shown to be required for proper tail regeneration and AP axis polarity in the flatworm *Schmidtea mediterranea*; in *Smed-tsh*-RNAi experiments, posteriorly amputated worms regenerated heads in place of tails, a phenotype also seen in planarian Wnt knockdown experiments (Owen, Wagner, Chen, Petersen, & Reddien, 2015). In the vertebrate model *Xenopus laevis*, inhibition of *Xlae-tshz3* has been shown to disrupt the DV axis, also reflecting its involvement with Wnt signaling (Onai et al., 2007). Moreover, the three copies of mouse *tshz* can rescue *tsh* null mutants of *D. melanogaster* (Manfroid, Caubit, Kerridge, & Fasano, 2004), and at least one of these is necessary for development of the ureter (Caubit et al., 2008). These fragmentary data may hint at a broader functional homology of *tio/tsh* homologs across Bilateria.

However, even within arthropods, the evolution of *tio/tsh* function is difficult to characterize; each of the three available data points for gene function (the insects *O. fasciatus*, *T. castaneum*, and *D. melanogaster*) have yielded unique spectra of phenocopies. The phenotype exhibited by *O. fasciatus* is difficult to compare to the fruit fly data, because only the distal leg morphology is affected, whereas the proximal

appendage territory and the body wall of the thoracic segments are not. Shippy et al. (2008) made a compelling case for the absence of a trunk selector function for the *T. castaneum tio/tsh* homolog, based on parental and embryonic RNAi data. One limitation of their interpretation is that the effectiveness of the knockdown was not directly assessed by Shippy et al. (2008) in *T. castaneum*. Indeed, we were able to replicate the embryonic RNAi phenotypes reported by (Herke et al., 2005) in *O. fasciatus*, and with much higher penetrance, by using parental RNAi against a larger *Ofas-tio/tsh* fragment (776 bp vs. 300 bp fragment used by (Herke et al., 2005), but our assessments of knockdown effectiveness using in situ hybridization showed that *Ofas-tio/tsh* expression was not fully abrogated by parental RNAi (data not shown; see also Setton et al., 2017 for comparably incomplete knockdown in *Ofas-ss*, in spite of a clear loss-of-function phenotype).

A rigorous test of the hypothesized trunk selector function for *tio/tsh* in arthropods should incorporate tests of mutagenesis in non-*Drosophila* insects to generate *tio/tsh* null mutants. Future work should also direct attention to functional interrogation of *tio/tsh* homologs in arachnids, toward understanding whether this gene family has retained conserved functions pertaining to appendage patterning.

ACKNOWLEDGMENTS

We are indebted to Jesus Ballesteros, Erik D. Nolan, Jill T. Oberski, Andrew Z. Ontano, and Carlos Santibañez López for assistance with dissection of embryos for gene expression assays and/or independent verification of phenotypes. Comments from Carlos Santibañez López and two anonymous reviewers improved an earlier draft of this manuscript. Assistance with collection and fixation of harvestman embryos for gene expression assays was provided by Audrey R. Crawford and Calvin So. A subset of the imaging was performed at the Newcomb Imaging Center, Department of Botany, UW-Madison. This work was supported by National Science Foundation grant IOS-1552610 to PPS.

ORCID

Prashant P. Sharma http://orcid.org/0000-0002-2328-9084

REFERENCES

Abu-Shaar, M., & Mann, R. S. (1998). Generation of multiple antagonistic domains along the proximodistal axis during *Drosophila* leg development. *Development*, *125*, 3821–3830.

Akiyama-Oda, Y., & Oda, H. (2003). Early patterning of the spider embryo: A cluster of mesenchymal cells at the cumulus produces Dpp signals received by germ disc epithelial cells. *Development*, *130*, 1735–1747.

Angelini, D., Liu, P., Hughes, C., & Kaufman, T. (2005). Hox gene function and interaction in the milkweed bug *Oncopeltus fasciatus* (Hemiptera). *Developmental Biology*, *287*, 440–455.

Casares, F., & Mann, R. S. (1998). Control of antennal versus leg development in *Drosophila*. *Nature*, *392*, 723–726.

Caubit, X., Lye, C. M., Martin, E., Coré, N., Long, D. A., Vola, C., … Fasano, L. (2008). Teashirt 3 is necessary for ureteral smooth muscle differentiation downstream of SHH and BMP4. *Development*, *135*, 3301–3310.

Cohen, S. M., Brönner, G., Küttner, F., Jürgens, G., & Jäckle, H. (1989). Distal-less encodes a homoeodomain protein required for limb development in *Drosophila*. *Nature*, *338*, 432–434.

Datta, R. R., Weasner, B. P., & Kumar, J. P. (2011). A dissection of the *teashirt* and *tiptop* genes reveals a novel mechanism for regulating transcription factor activity. *Developmental Biology*, *360*, 391–402.

Denholm, B., Hu, N., Fauquier, T., Caubit, X., Fasano, L., & Skaer, H. (2013). The *tiptop/teashirt* genes regulate cell differentiation and renal physiology in *Drosophila*. *Development*, *140*, 1100–1110.

Dong, P. D., Chu, J., & Panganiban, G. (2001). Proximodistal domain specification and interactions in developing *Drosophila* appendages. *Development*, *128*, 2365–2372.

Dong, P. D. S., Dicks, J. S., & Panganiban, G. (2002). Distal-less and homothorax regulate multiple targets to pattern the *Drosophila* antenna. *Development*, *129*, 1967–1974.

Duncan, D. M., Burgess, E. A., & Duncan, I. (1998). Control of distal antennal identity and tarsal development in Drosophila by spineless-aristapedia, a homolog of the mammalian dioxin receptor. *Genes & Development*, *12*, 1290–1303.

Edgar, R. C. (2004). MUSCLE: multiple sequence alignment with high accuracy and high throughput. *Nucleic Acids Research*, *32*, 1792–1797.

Emerald, B., & Cohen, S. (2004). Spatial and temporal regulation of the homeotic selector gene Antennapedia is required for the establishment of leg identity in *Drosophila*. *Developmental Biology*, *267*, 462–472.

Emmons, R. B., Duncan, D., & Duncan, I. (2007). Regulation of the *Drosophila* distal antennal determinant spineless. *Developmental Biology*, *302*, 412–426.

Fasano, L., Röder, L., Coré, N., Alexandre, E., & Vola, C. (1991). The gene *teashirt* is required for the development of *Drosophila* embryonic trunk segments and encodes a protein with widely spaced zinc finger motifs. *Cell*, *64*, 63–79.

Herke, S. W., Serio, N. V., & Rogers, B. T. (2005). Functional analyses of *tiptop* and *Antennapedia* in the embryonic development of *Oncopeltus fasciatus* suggests an evolutionary pathway from ground state to insect legs. *Development*, *132*, 27–34.

Hughes, C. L., & Kaufman, T. C. (2002). Exploring the myriapod body plan: Expression patterns of the ten Hox genes in a centipede. *Development*, *129*, 1225–1238.

Janssen, R., Eriksson, B. J., Budd, G. E., Akam, M., & Prpic, N.-M. (2010). Gene expression patterns in an onychophoran reveal that regionalization predates limb segmentation in pan-arthropods. *Evolution & Development*, *12*, 363–372.

Kadner, D., & Stollewerk, A. (2004). Neurogenesis in the chilopod *Lithobius forficatus* suggests more similarities to chelicerates than to insects. *Development Genes and Evolution*, *214*, 367–379.

Kao, D., Lai, A. G., Stamataki, E., Rosic, S., Konstantinides, N., Jarvis, E., … Aboobaker, A. (2016). The genome of the crustacean *Parhyale hawaiensis*, a model for animal development, regeneration, immunity and lignocellulose digestion. *Elife*, *5*, 1.

Khadjeh, S., Turetzek, N., Pechmann, M., Schwager, E. E., Wimmer, E. A., Damen, W. G. M., & Prpic, N.-M. (2012). Divergent role of the Hox gene *Antennapedia* in spiders is responsible for the convergent evolution of abdominal limb repression. *Proceedings of the National Academy of Sciences of the United States of America*, *109*, 4921–4926.

Kuzin, B., Doszhanov, K., & Mazo, A. (1997). Interaction between *spineless-aristapedia* gene and genes from *Antennapedia* and *bithorax* complexes of *Drosophila melanogaster*. *The International Journal of Developmental Biology*, *41*, 867–875.

Laugier, E., Yang, Z., Fasano, L., Kerridge, S., & Vola, C. (2005). A critical role of *teashirt* for patterning the ventral epidermis is masked by ectopic expression of *tiptop*, a paralog of *teashirt* in *Drosophila*. *Developmental Biology*, *283*, 446–458.

Le, S. Q., Dang, C. C., & Gascuel, O. (2012). Modeling protein evolution with several amino acid replacement matrices depending on site rates. *Molecular Biology and Evolution*, *29*, 2921–2936.

Liu, P., & Kaufman, T. C. (2009a). Morphology and husbandry of the large milkweed bug, *Oncopeltus fasciatus*. *CSH Protocols*, *4*(8), pdb.emo127.

Liu, P., & Kaufman, T. C. (2009b). Dissection and fixation of large milkweed bug (*Oncopeltus*) embryos. *CSH Protocols*, *4*(8), pdb.prot5261.

Liu, P., & Kaufman, T. C. (2009c). In situ hybridization of large milkweed bug (*Oncopeltus*) tissues. *CSH Protocols*, *4*(8), pdb.prot5262.

Liubicich, D. M., Serano, J. M., Pavlopoulos, A., Kontarakis, Z., Protas, M. E., Kwan, E., … Patel, N. H. (2009). Knockdown of Parhyale Ultrabithorax recapitulates evolutionary changes in crustacean appendage morphology. *Proceedings of the National Academy of Sciences of the United States of America*, *106*, 13892–13896.

Manfroid, I., Caubit, X., Kerridge, S., & Fasano, L. (2004). Three putative murine Teashirt orthologues specify trunk structures in *Drosophila* in the same way as the *Drosophila teashirt* gene. *Development*, *131*, 1065–1073.

Mardon, G., Solomon, N. M., & Rubin, G. M. (1994). *dachshund* encodes a nuclear protein required for normal eye and leg development in *Drosophila*. *Development*, *120*, 3473–3486.

Martin, A., Serano, J. M., Jarvis, E., Bruce, H. S., Wang, J., Ray, S., … Patel, N. H. (2016). CRISPR/Cas9 mutagenesis reveals versatile roles of Hox genes in crustacean limb specification and evolution. *Current Biology*, *26*, 14–26.

Onai, T., Matsuo-Takasaki, M., Inomata, H., Aramaki, T., Matsumura, M., Yakura, R., … Sasai, Y. (2007). XTsh3 is an essential enhancing factor of canonical Wnt signaling in *Xenopus* axial determination. *The EMBO Journal*, *26*, 2350–2360.

Owen, J. H., Wagner, D. E., Chen, C.-C., Petersen, C. P., & Reddien, P. W. (2015). Teashirt is required for head-versus-tail regeneration polarity in planarians. *Development*, *142*, 1062–1072.

Panfilio, K., Vargas Jentzsch, I. M., Benoit, J. B., Erezyilmaz, D., Suzuki, Y., Colella, S., … Richards, S. (2017). Molecular evolutionary trends and feeding ecology diversification in the Hemiptera, anchored by the milkweed bug genome. *biorxiv*, https://doi.org/10.1101/201731.

Panganiban, G., Irvine, S. M., Lowe, C., Roehl, H., Corley, L. S., Sherbon, B., … Carroll, S. B. (1997). The origin and evolution of animal appendages. *Proceedings of the National Academy of Sciences of the United States of America*, *94*, 5162–5166.

Panganiban, G., Nagy, L., & Carroll, S. B. (1994). The role of the *Distal-less* gene in the development and evolution of insect limbs. *Current Biology*, *4*, 671–675.

Panganiban, G., Sebring, A., Nagy, L., & Carroll, S. B. (1995). The development of crustacean limbs and the evolution of arthropods. *Science*, *270*, 1363–1366.

Pavlopoulos, A., Kontarakis, Z., Liubicich, D. M., Serano, J. M., Akam, M., Patel, N. H., & Averof, M. (2009). Probing the evolution of appendage specialization by Hox gene misexpression in an emerging model crustacean. *Proceedings of the National Academy of Sciences of the United States of America*, *106*, 13897–13902.

Pechmann, M., Schwager, E. E., Turetzek, N., & Prpic, N.-M. (2015). Regressive evolution of the arthropod tritocerebral segment linked to functional divergence of the Hox gene *labial*. *Proceedings of the Royal Society of London B*, *282*, 20151162.

Peterson, M. D., Rogers, B. T., Popadic, A., & Kaufman, T. C. (1999). The embryonic expression pattern of labial, posterior homeotic complex genes and the teashirt homologue in an apterygote insect. *Development Genes and Evolution*, *209*, 77–90.

Posnien, N., Zeng, V., Schwager, E. E., Pechmann, M., Hilbrant, M., Keefe, J. D., … Extavour, C. G. (2014). A comprehensive reference transcriptome resource for the common house spider *Parasteatoda tepidariorum*. *PLoS ONE*, *9*, e104885.

Prpic, N.-M., Janssen, R., Wigand, B., Klingler, M., & Damen, W. G. M. (2003). Gene expression in spider appendages reveals reversal of *exd/hth* spatial specificity, altered leg gap gene dynamics, and suggests divergent distal morphogen signaling. *Developmental Biology*, *264*, 119–140.

Ronco, M., Uda, T., Mito, T., Minelli, A., Noji, S., & Klingler, M. (2008). Antenna and all gnathal appendages are similarly transformed by *homothorax* knock-down in the cricket *Gryllus bimaculatus*. *Developmental Biology*, *313*, 80–92.

Röder, L., Vola, C., & Kerridge, S. (1992). The role of the *teashirt* gene in trunk segmental identity in *Drosophila*. *Development*, *115*, 1017–1033.

Santos, J. S., Fonseca, N. A., Vieira, C. P., Vieira, J., & Casares, F. (2010). Phylogeny of the teashirt-related zinc finger (tshz) gene family and analysis of the developmental expression of *tshz2* and *tshz3b* in the zebrafish. *Developmental Dynamics*, *239*, 1010–1018.

Schoppmeier, M., & Damen, W. G. (2001). Double-stranded RNA interference in the spider *Cupiennius salei*: the role of *Distal-less* is evolutionarily conserved in arthropod appendage formation. *Development Genes and Evolution*, *211*, 76–82.

Schwager, E. E., Sharma, P. P., Clarke, T., Leite, D. J., Wierschin, T., Pechmann, M., … McGregor, A. P. (2017). The house spider genome reveals an ancient whole-genome duplication during arachnid evolution. *BMC Biology*, *15*, 62.

Setton, E. V. W., & Sharma, P. P. (2018). Cooption of an appendage-patterning gene cassette in the head segmentation of arachnids. *Proceedings of the National Academy of Sciences of the United States of America*, *115*, E3491–E3500.

Setton, E. V. W., March, L. E., Nolan, E. D., Jones, T. E., Cho, H., Wheeler, W. C., … Sharma, P. P. (2017). Expression and function of *spineless* orthologs correlate with distal deutocerebral appendage morphology across Arthropoda. *Developmental Biology*, *430*, 224–236.

Sharma, P. P. (2017). Chelicerates and the conquest of land: A view of arachnid origins through an evo-devo spyglass. *Integrative and Comparative Biology*, *57*, 510–522.

Sharma, P. P., Kaluziak, S. T., Perez-Porro, A. R., Gonzalez, V. L., Hormiga, G., Wheeler, W. C., & Giribet, G. (2014a). Phylogenomic interrogation of Arachnida reveals systemic conflicts in phylogenetic signal. *Molecular Biology and Evolution*, *31*, 2963–2984.

Sharma, P. P., Schwager, E. E., Extavour, C. G., & Giribet, G. (2012a). Evolution of the chelicera: A *dachshund* domain is retained in the deutocerebral appendage of Opiliones (Arthropoda, Chelicerata). *Evolution & Development*, *14*, 522–533.

Sharma, P. P., Schwager, E. E., Extavour, C. G., & Giribet, G. (2012b). Hox gene expression in the harvestman *Phalangium opilio* reveals divergent patterning of the chelicerate opisthosoma. *Evolution & Development*, *14*, 450–463.

Sharma, P. P., Schwager, E. E., Extavour, C. G., & Wheeler, W. C. (2014b). Hox gene duplications correlate with posterior heteronomy in scorpions. *Proceedings of the Royal Society of London B*, *281*, 20140661.

Sharma, P. P., Tarazona, O. A., Lopez, D. H., Schwager, E. E., Cohn, M. J., Wheeler, W. C., & Extavour, C. G. (2015). A conserved genetic mechanism specifies deutocerebral appendage identity in insects and arachnids. *Proceedings of the Royal Society of London B*, *282*, 20150698.

Shippy, T. D., Tomoyasu, Y., Nie, W., Brown, S. J., & Denell, R. E. (2008). Do *teashirt* family genes specify trunk identity? Insights from the single *tiptop/teashirt* homolog of *Tribolium castaneum*. *Development Genes and Evolution*, *218*, 141–152.

Shippy, T. D., Yeager, S. J., & Denell, R. E. (2008). The *Tribolium spineless* ortholog specifies both larval and adult antennal identity. *Development Genes and Evolution*, *219*, 45–51.

Stamatakis, A. (2014). RAxML version 8: A tool for phylogenetic analysis and post-analysis of large phylogenies. *Bioinformatics*, *30*, 1312–1313.

Stamatakis, A., Hoover, P., & Rougemont, J. (2008). A rapid bootstrap algorithm for the RAxML web servers. *System Biology*, *57*, 758–771.

Struhl, G. (1982a). Genes controlling segmental specification in the *Drosophila* thorax. *Proceedings of the National Academy of Sciences of the United States of America*, *79*, 7380–7384.

Struhl, G. (1982b). *Spineless-aristapedia*: A homeotic gene that does not control the development of specific compartments in *Drosophila*. *Genetics*, *102*, 737–749.

Struhl, G., & White, R. (1985). Regulation of the *Ultrabithorax* gene of *Drosophila* by other bithorax complex genes. *Cell*, *43*, 507–519.

Toegel, J. P., Wimmer, E. A., & Prpic, N.-M. (2009). Loss of *spineless* function transforms the *Tribolium* antenna into a thoracic leg with pretarsal, tibiotarsal, and femoral identity. *Development Genes and Evolution*, *219*, 53–58.

Tomoyasu, Y., Arakane, Y., Kramer, K. J., & Denell, R. E. (2009). Repeated co-options of exoskeleton formation during wing-to-elytron evolution in beetles. *Current Biology*, *19*, 2057–2065.

Wang, W., Tindell, N., Yan, S., & Yoder, J. H. (2013). Homeotic functions of the Teashirt transcription factor during adult *Drosophila* development. *Biology Open*, *2*, 18–29.

SUPPORTING INFORMATION

Additional supporting information may be found online in the Supporting Information section at the end of the article.

How to cite this article: March LE, Smaby RM, Setton EVW, Sharma PP. The evolution of selector gene function: Expression dynamics and regulatory interactions of *tiptop/teashirt* across Arthropoda. *Evolution & Development*. 2018;20:219–232. https://doi.org/10.1111/ede.12270